物理化学学报(*Wuli Huaxue Xuebao*)

March   *Acta Phys. -Chim. Sin.*, **2008**, 24(3)：359−363   359

以阴离子多肽为模板合成二氧化硅纳米空心球

李丽颖[1]   王金桂[1]   孙平川[1]   刘晓航[1]   丁大同[2]   陈铁红[1,*]

([1]南开大学化学学院材料化学系, 教育部功能高分子材料重点实验室, 天津 300071; [2]南开大学物理学院, 天津 300071)

摘要： 以聚阴离子多肽(聚谷氨酸钠)控制合成了微孔二氧化硅空心球. 在合成过程中, 以3-氨丙基三甲氧基硅烷(APMS)和正硅酸乙酯(TEOS)为硅源, 聚谷氨酸钠为模板. 硅源与阴离子多肽模板之间的组装依照以阴离子表面活性剂为模板剂组装合成介孔二氧化硅的机理, 即 S⁻N⁺I⁻机理, 其中 S 表示阴离子多肽, I 表示 TEOS, N 表示共结构导向剂 APMS. 组装过程中质子化的 APMS 与阴离子多肽之间形成静电相互作用, 同时, AMPS 和 TEOS 共同水解聚合形成围绕阴离子多肽模板的二氧化硅骨架, 多肽的二级结构为微孔孔道的模板. 以阴离子多肽为模板可以在不同的实验条件下控制微孔纳米空心球, 微孔亚微米空心球和实心球形貌的合成. 在生物矿化过程中, 阴离子多肽往往控制碳酸钙或磷酸钙的沉积, 而我们的实验结果表明, 在适当的硅源存在下, 阴离子多肽也可以诱导二氧化硅的沉积.

关键词： 阴离子聚氨基酸; 聚谷氨酸钠; 微孔; 二氧化硅; 空心纳米球

中图分类号： O648

Microporous Silica Hollow Nanospheres Templated by Anionic Polypeptide

LI Li-Ying[1]   WANG Jin-Gui[1]   SUN Ping-Chuan[1]   LIU Xiao-Hang[1]
DING Da-Tong[2]   CHEN Tie-Hong[1,*]

([1]*Key Laboratory of Functional Polymer Materials of the Ministry of Education, Department of Materials Chemistry, College of Chemistry, Nankai University, Tianjin 300071, P. R. China; [2]College of Physics, Nankai University, Tianjin 300071, P. R. China*)

Abstract： Anionic polypeptide, the poly(sodium L-glutamate), was applied to fabricate microporous silica hollow nanospheres templated by the secondary structures of the polypeptide as porogens. In the synthesis, 3-aminopropyltrimethoxysilane (APMS) and tetraethyl orthosilicate (TEOS) were used as the silica sources, and the coassembly followed the mechanism of the anionic surfactant-templated mesoporous silica (AMS) through a S⁻N⁺I⁻ pathway，where S indicates the anionic polypeptide，I indicates inorganic precursors (TEOS), and N indicates costructure-directing agent (APMS), which interacted with the negatively charged anionic polypeptide secondary structures electrostatically and cocondensed with silica source to form the silica framework. The product was subjected to characterizations of X-ray diffraction (XRD), infrared (IR) spectroscopy, thermogravimetric (TG) analysis, scanning electron microscopy (SEM), transmitted electron microscopy (TEM), and nitrogen adsorption-desorption measurement. It was found that the pH value of the synthesis solution was an important factor to the morphological control of the silica products. Besides the microporous hollow nanospheres, microporous submicron silica solid and hollow spheres were also obtained facilely by changing the synthesis parameters. Our study further implied that anionic polypeptides, which were able to control mineralization of calcium carbonate and calcium phosphate, could also induce silica condensation in the presence of proper silica precursors. It was also expected that functional calcium carbonate (phosphate)/silica-nanocomposite materials would be fabricated under the control of the anionic polypeptide.

Key Words： Anionic polypeptide; Poly(sodium L-glutamate); Microporous; Silica; Hollow nanospheres

Silica materials with well-defined morphology, microporosity and mesoporosity, are of interest for various applications, such as catalysis, separation, and drug delivery. Cationic surfactants and polymeric surfactants have been widely applied in the fabrication of mesoporous silica[1-4]. Inspired by the biosilicification in nature, a set of cationic proteins (e.g. silaffins and silicateins) extracted from diatoms and synthetic polyamines (e.g. poly-L-lysine) have been applied to promote and to mediate the silica condensation *in vitro*[5,6]. Cha *et al.*[7] demonstrated that the synthetic cysteine-lysine block copolypeptides could direct the assembly of silica particles with controllable morphologies. Shantz *et al.*[8] firstly proposed that the secondary structures, such as α-helices and β-sheets of the poly-L-lysine, could be used to template microporous silica. Triblock copolymer poly (L-phenylalanine)-b-poly(ethylene glycol)-b-poly(L-phenylalanine) was used as a template, and through the $\pi-\pi$ interaction between the phenyl groups of the poly(L-phenylalanine) and the anilino-methyl triethoxy silane, hierarchically structured silica with micropores and interconnected layers of macropores was fabricated[9,10].

Recently, Che *et al.*[11] firstly reported the synthesis of highly ordered anionic surfactant-templated mesoporous silica (AMS) materials using anionic surfactant and costructure-directing agent (CSDA) through an S^-N^+-I^- pathway, where S indicates surfactant, I indicates inorganic precursors, and N indicates CSDA (e.g. APMS), which interacts with the negatively charged anionic surfactants electrostatically and is cocondensed with silica source to form the silica framework. This new synthetic route has been proven to be a successful way for the formation of a series of novel mesostructured phases[12,13], as well as for the hierarchical morphologies[14]. Highly acidic glycoproteins are rich in aspartate and glutamate and can control the mineralization of calcium carbonate and calcium phosphate[15]. Acidic polypeptide was also used to synthesize nanoporous alumina[16]. However, anionic polypeptide has never been reported to control the condensation of silica. We report that anionic polypeptide, the poly (sodium L-glutamate), can be applied for the synthesis of microporous silica hollow nanospheres with the secondary structures of the polypeptide as porogens inspired by the templating pathway of the anionic surfactants[11]. APMS interacted electrostatically with the negatively charged polypeptide chain and was cocondensed with TEOS to form the silica framework. Thus, microporous silica hollow nanospheres and submicron silica solid and hollow spheres were obtained.

1 Experimental

The synthesis of poly(γ-benzyl-L-glutamate) was performed according to our previous study[17]. Poly(sodium L-glutamate) was obtained according to the procedure of the literature [18]. By ^{1}H NMR analysis, the average molecular weight of the poly(sodium L-glutamate) is found to be ca 6000. In a typical synthesis of the silica hollow nanospheres, 80 mg poly(sodium L-glutamate) was dissolved in 30 mL deionized water under stirring at 30 ℃. A few drops of 0.1 mol·L^{-1} HCl solution were then added under vigorous stirring to adjust the pH to 6.0. After vigorous stirring

for 1 h at room temperature, a mixture of 0.35 g TEOS and 0.07 g APMS (Acros Organics) was added under vigorous stirring, and the pH value was shifted to 8.8 as a result of the addition of APMS. The mixture solution was left static for 2 h and was then transferred to an 80 ℃ oven to react for 21 h statically. The white precipitate was centrifugated, washed with deionized water, and dried at 50 ℃. The templates were removed by calcination at 550 ℃ for 6 h. The synthesis was performed similar to the above procedure but without the addition of the polypeptide and this silica sample was used as comparison with those silica samples synthesized with the polypeptide. The synthesis procedure of the submicron silica solid spheres was similar to that of the hollow nanospheres, except that extra 1.0 g 0.1 mol·L^{-1} HCl solution was added to the polypeptide solution to tune the pH value to 4.5 before the addition of APMS and TEOS. For the submicron silica hollow spheres, the synthesis was similar as that of the solid spheres except that the amount of AMPS was reduced to 0.035 g.

Scanning electron microscopy (SEM) images were measured on a Shimadzu SS-550 scanning electron microscope working at 15 kV. The TEM observations were performed on a Philips Tecnai F20 microscope. The samples were dispersed in ethanol by sonication and were subsequently dropped on copper grids. Thermogravimetry (TG) analyses were performed with a Rigaku TG-DTA analyzer at a linear heating rate of 20 ℃·min^{-1}, and α-Al$_2$O$_3$ was used as a reference. Fourier transformation infrared (FT-IR) transmission spectra were recorded using a Brucker VECTOR 22 spectrometer. Powder X-ray diffraction pattern was recorded using a Rigaku D/max-2500 diffractometer, with Cu K_α radiation (λ=0.154 nm) at a scanning rate of 0.01 (°)·s^{-1}. Nitrogen adsorption and desorption isotherms were measured on a BELSORP mini II sorption analyzer at 77 K. Surface area was calculated by the Brunauer-Emmett-Teller (BET) method, and pore-size distribution was calculated by micropore analysis (MP) method.

2 Results and discussion

At pH 6.0, the solution of poly(sodium L-glutamate) was clear. As the pK_α of the glutamic acid is approximately 2; thus, at pH 6.0, most of the carboxyl groups in the poly(L-glutamate) should be negatively charged in the solution. After addition of APMS and TEOS, the solution gradually became turbid, and finally a white suspension was obtained. The XRD pattern of the synthesized silica (not shown) is featureless, indicating a total amorphous structure. The SEM image of the calcined product is shown in Fig.1a in which small particles can be observed. The TEM images display that the product is composed of dispersed hollow nanospheres, with the average size of 170 nm. It can be noticed that the contour of the inner empty space of the nanospheres is not regular. Larger spheres possess larger interior empty space, whereas the shell thicknesses are nearly the same (ca 50 nm). High resolution TEM (HRTEM) image of the nanospheres displays a porous shell (Fig.1d), which is confirmed by the N$_2$ adsorption-desorption measurement (discussed later).
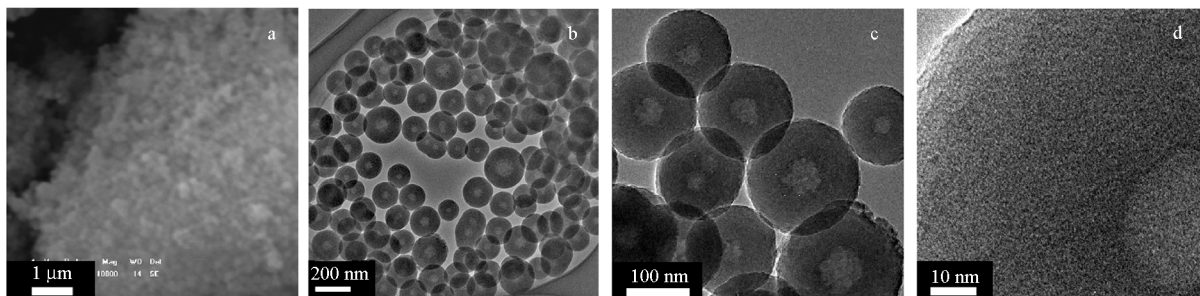
Fig.1   SEM (a) and TEM (b, c, and d) images of the hollow nanospheres

The IR spectrum of the poly(sodium L-glutamate) (Fig.2a) displays two characteristic vibration bands at 1652 and 1556 cm^{-1}, which could be assigned to the amide I and II bands of the polypeptide, respectively, indicating the presence of α-helix secondary structures according to the literature[19,20]. In the IR spectrum of the as-synthesized silica hollow nanospheres (Fig.2b), the bands at 1652 and 1556 cm^{-1} are still present. It should be noticed that the physically adsorbed water would give rise to a vibration band at approximately 1650 cm^{-1}, and as shown in the IR spectrum of the calcined silica hollow nanospheres (Fig.2e), there appears a weak peak at 1637 cm^{-1}, which was ascribed to the physically adsorbed water, probably in the micropores (see below the N$_2$ adsorption-desorption measurement). In Fig.2b, the physically adsorbed water could also contribute partly to the IR band at 1652 cm^{-1} because in the IR spectrum of the pure polypeptide (Fig.2a), the 1556 cm^{-1} peak is slightly stronger than the 1652 cm^{-1} peak, whereas in the as-synthesized samples (see also Fig.2 (b, c, d), discussed later), the intensities of the two bands are almost the same. However, the presence of the 1556 cm^{-1} band provides unambiguous proof that the polypeptide with the α-helix secondary structures was included in the as-synthesized samples.

As APMS was involved in the synthesis, the aminopropyl groups would remain in the as-prepared silica. For the as-synthesized silica without the addition of polypeptide, the TG analysis (Fig.3a) indicates the total mass loss of approximately 9% (mass fraction, w), mainly corresponding to the decomposition of the organic groups. From the TG curve of the as-synthesized silica

hollow nanospheres (Fig.3b), the mass loss is increased to approximately 22% (w), indicating again the inclusion of the polypeptide.

It has been proposed that the α-helix secondary structures of poly-L-lysine could be used to template cylindrical micropores[8]. In this study, N$_2$ adsorption isotherm of the hollow silica nanospheres displays a type I curve (Fig.4A(a)), indicating the presence of microporosity in the calcined silica. The upturn of the adsorption after p/p_0=0.9 could be due to the empty inner space of the hollow nanospheres and the voids between the hollow nanospheres. The BET specific surface area is 161 m$^2\cdot$g^{-1}, with a microporous pore volume of 0.07 cm$^3\cdot$g^{-1} by t-plot analysis. The micropore could be due to the presence of the polypeptide because if no polymer was added in the synthesis, only nonporous silica particles were obtained (data are not shown).

At pH 6.0, a small part of the side-chain carboxyl groups would be protonated by the addition of acid, and the hydrophobic characteristic of the polymer chain might be increased. This may give rise to the formation of nanosized colloidal particles by some aggregated polymer chains. After the addition of the silica source (APMS and TEOS), silicate species after hydrolysis of the silica precursors would penetrate and interact with the anionic polypeptide colloidal particles. The protonated APMS interacted electrostatically with the negatively charged polypeptide chain and cocondensed with TEOS to form the silica framework (Scheme 1a). This coassembly between polypeptide and the silica precursors started from the outside of the polypeptide colloidal particles and gradually extended inside. At relatively high-
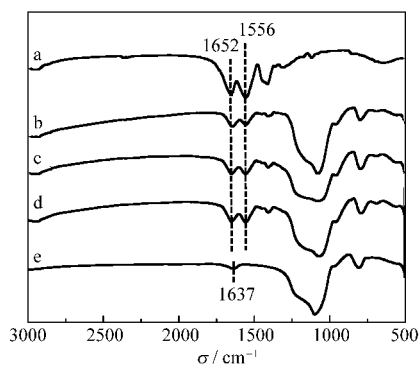

Fig.2   IR spectra of different samples

(a) poly(sodium L-glutamate), (b) as-synthesized hollow silica nanospheres,
(c) submicron solid silica spheres, (d) submicron hollow silica spheres,
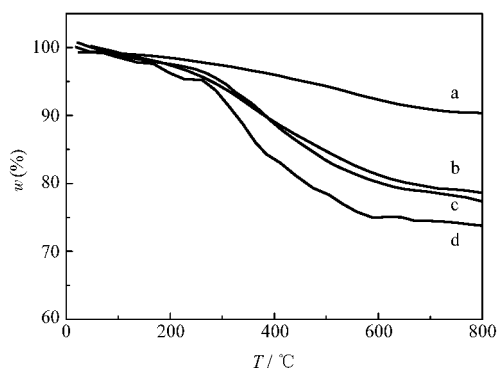(e) calcined hollow silica nanospheres

Fig.3   TG analyses of different samples

(a) as-prepared silica without addition of poly(sodium L-glutamate),
(b) silica hollow nanospheres, (c) submicron silica solid spheres,
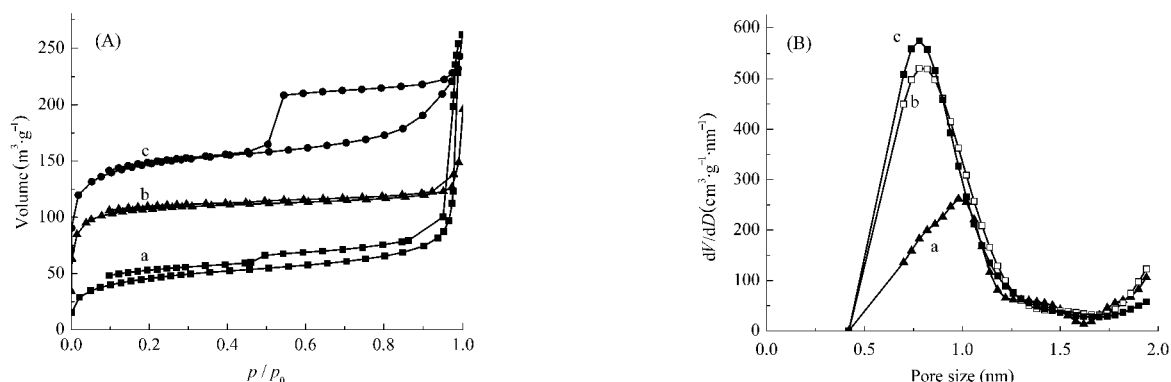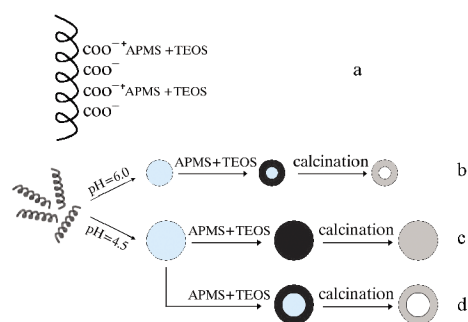(d) submicron silica hollow spheres

Fig.4   N₂ adsorption-desorption isotherms (A) and pore size distribution curves by MP method (B) of different samples
(a) silica hollow nanospheres, (b) submicron silica solid spheres, (c) silica hollow spheres; Line c in the figure (A) is up-shifted by 40 cm³·g⁻¹ for clarity.

er pH, there were less positively charged APMSs; thus, there were less interaction sites between the anionic template and the APMS[13]. This would induce less involvement of the polypeptide in the hybrid silica, giving rise to lower porosity and relatively low surface area (161 m²·g⁻¹). The condensation of the silica would hinder the diffusion of the silica species inside the polypeptide colloids and thus leave an uninteracted core of the polypeptides, giving rise to the morphology of hollow spheres (Scheme 1b). The irregular contour of the inner empty core could be explained by an uneven coassembly process occurred from the outside to the inside of the colloidal polymer particles.

To test our speculation on the formation mechanism of the hollow nanospheres, a control experiment was also performed. During the synthesis, before the addition of APMS and TEOS, additional 1.0 g 0.1 mol·L⁻¹ HCl solution was added to the polypeptide solution, and the pH was decreased to 4.5. Addition of more acid could result in the following two effects. (i) Larger colloidal particles of poly (L-glutamate) chains formed due to the higher hydrophobic property of the chains because more carboxyl groups were protonated by the acid. This was proved by the phenomenon that the clear solution became foggy or pale white immediately after addition of the acid, probably due to the formation of larger colloidal particles of aggregated polymer chains.   (ii) At lower pH, there were more interaction sites be-

tween the carboxyl side-groups and protonated APMS. This would favor the coassembly of the templates and the silica precursors[13].

The SEM image of the product obtained with more acid displays larger spheres (Fig.5a) with the average size of 380 nm. The TEM images (Fig.5(b, c, d)) indicate that the spheres are solid and porous. The IR spectrum (Fig.2c) is similar to the hollow nanospheres, showing the presence of the α-helix secondary structures. The TG analysis (Fig.3c) indicates a mass loss of approximately 23% (*w*). The N₂ adsorption-desorption curve is a type I isotherm, and the *t*-plot is typically microporous (Fig.4B(b)). The solid spheres have much higher surface area of 400 m²·g⁻¹ and pore volume of 0.23 cm³·g⁻¹ (microporous pore volume of 0.17 cm³·g⁻¹). From TEM images, there occasionally appeared spheres with a small empty core, indicating that the formation process of the solid spheres resembles the hollow nanospheres, i.e.,

Scheme 1   Assembly pathway of the anionic polypeptide and the protonated APMS (a) and tentative formation mechanisms of the hollow nanospheres (b), submicron solid spheres (c), and submicron hollow spheres (d) tuned by different amounts of acid and APMS
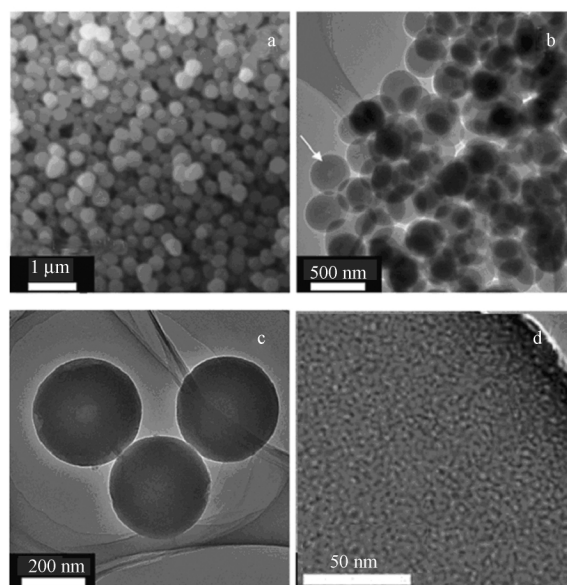

Fig.5   SEM (a) and TEM (b, c, d) images of the solid spheres synthesized with the addition of more acid
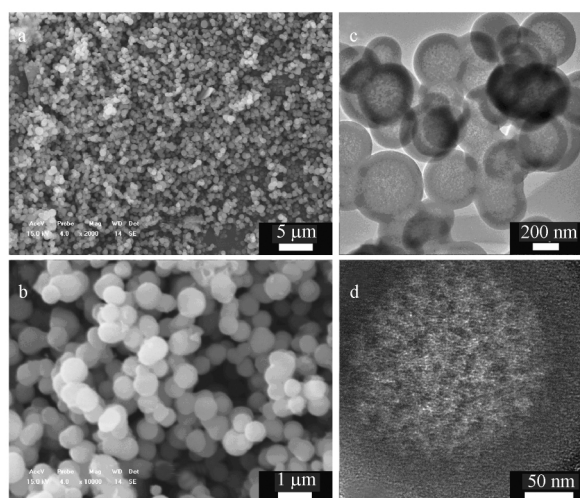The arrow in the figure b indicates a sphere with an empty core.

Fig.6   SEM (a, b) and TEM (c, d) images of the calcined submicron hollow spheres

the silica precursors could penetrate into the colloidal particles of the polypeptide and coassembly together. Although at lower pH the colloidal particles of the polymers were larger, more APMSs were positively charged to induce more interaction sites between the —COO⁻ and ⁺APMS, favoring the coassembly between the templates and the silica precursors. This would give rise to solid silica spheres, without unreacted polymer inside as the core (Scheme 1c). Inclusion of more polymers in the silica hybrid would also induce a higher porosity.

It is interesting to note that the morphology of the submicron solid spheres could be further tuned by altering the amount of APMS. After adjusting the pH of the polypeptide solution to 4.5 by acid, if the amount of AMPS was reduced from 0.07 g to 0.035 g, then the silica hollow spheres with an average diameter of 550 nm was obtained (Fig.6). The IR spectrum (Fig.2d) is similar to those of the hollow nanospheres and the solid submicron spheres, and the mass loss was increased to 27% (w), probably due to the presence of the residual polypeptide template inside the core. The thickness of the shell is approximately 70 nm and is almost same irrespective to the size of the hollow spheres. The TEM image (Fig.6d) shows that the shell is also porous, which was confirmed by the N_2 adsorption measurement. The N_2 adsorption-desorption curve is a type I isotherm (Fig.4c). The large hysteresis loop could be ascribed to the empty space of the hollow spheres. The BET surface area is 350 $m^2 \cdot g^{-1}$, and the pore volume is 0.29 $cm^3 \cdot g^{-1}$ (microporous pore volume of 0.14 $cm^3 \cdot g^{-1}$). The formation of the hollow spheres could be tentatively described by Scheme 1d, in which due to the reduced amount of the AMPS, there are not enough silica precursors to penetrate and to coassemble with the polypeptide colloidal particles; thus, an uninteracted core remained to give rise to the hollow morphology.

3   Conclusions

In summary, anionic polymer, the poly(sodium L-glutamate), was applied for the synthesis of microporous silica hollow

nanospheres with the secondary structure of the polypeptide as porogens. The morphology of the microporous silica can be tuned from hollow nanospheres to submicron solid and hollow spheres by adjusting the synthesis parameters. Our study further implies that anionic polypeptides, which are able to control mineralization of calcium carbonate and calcium phosphate, could also induce silica condensation in the presence of proper silica precursors. It is also expected that functional calcium carbonate (phosphate)/silica nanocomposite materials would be fabricated under the control of the anionic polypeptide, and this study is in progress in our laboratory.

References

1   Kresge, C. T.; Leonowicz, M. E.; Roth, W. J.; Vartuli, J. C.; Beck, J. S. *Nature,* **1992, 359**: 710

2   Liu, L.; Zhang, G. Y.; Dong, J. X. *Acta Phys. -Chim. Sin.,* **2004, 20**(1): 65 [刘　雷, 张高勇, 董晋湘. 物理化学学报, **2004, 20**(1): 65]

3   Zhou, L. H.; Zhang, L. Z.; Hu, J.; Zhao, X. G.; Liu, H. L. *Acta Phys. -Chim. Sin.,* **2007, 23**(4): 620 [周丽绘, 张利中, 胡　军, 赵秀阁, 刘洪来. 物理化学学报, **2007, 23**(4): 620]

4   Zhao, C. X.; Chen, W.; Liu, Q.; Tian, G. *Acta Phys. -Chim. Sin.,* **2006, 22**(10): 1201 [赵春霞, 陈　文, 刘　琦, 田　高. 物理化学学报, **2006, 22**(10): 1201]

5   Sumper, M. *Science,* **2002, 295**: 2430

6   Cha, J. N.; Birkedal, H.; Euliss, L. E.; Bartl, M. H.; Wong, M. S.; Deming, T. J.; Stucky, G. D. *J. Am. Chem. Soc.,* **2003, 125**: 8285

7   Cha, J. N.; Stucky, G. D.; Morse, D. E.; Deming, T. J. *Nature,* **2000, 403**: 289

8   Hawkins, K. M.; Wang, S.; Ford, D.; Shantz, D. F. *J. Am. Chem. Soc.,* **2004, 126**: 9112

9   Liu, Y.; Shen, Z.; Li, L.; Sun, P.; Zhou, X.; Li, B.; Jin, Q.; Ding, D.; Chen, T. *Micro. Meso. Mater.,* **2006, 92**: 189

10 Liu, Y.; Zhou, H.; Shen, Z.; Li, L.; Zhou, X.; Sun, P.; Yuan, Z.; Chen, T.; Li, B.; Ding, D. *Chin. Sci. Bull.,* **2006, 51**: 493

11 Che, S.; Garcia-Bennett, A. E.; Yokoi, T.; Sakamoto, K.; Kunieda, H.; Terasaki, O.; Tatsumi, T. *Nat. Mater.,* **2003, 2**: 801

12 Che, S.; Liu, Z.; Ohsuna, T.; Sakamoto, K.; Terasaki, O.; Tatsumi, T. *Nature,* **2004, 429**: 281

13 Gao, C.; Qiu, H.; Zeng, W.; Sakamoto, Y.; Terasaki, O.; Sakamoto, K.; Chen, Q.; Che, S. *Chem. Mater.,* **2006, 18**: 3904

14 Wang, J.; Xiao, Q.; Zhou, H.; Sun, P.; Yuan, Z.; Li, B.; Ding, D.; Shi, A.; Chen, T. *Adv. Mater.,* **2006, 18**: 3284

15 Mann, S. Biomineralization: principles and concepts in bioinorganic materials chemistry. Oxford: Oxford University Press, 2001

16 Jan, J. S.; Shantz, D. F. *Chem. Commun.,* **2005**, (16): 2137

17 Li, L. Y.; Sun, P. C.; Yao, Y.; Chen, T. H.; Li, B. H.; Jin, Q. H.; Ding, D. T. *Chem. J. Chin. Univ.,* **2005, 26**: 1548 [李丽颖, 孙平川, 要　旸, 陈铁红, 李宝会, 金庆华, 丁大同. 高等学校化学学报, **2005, 26**: 1548]

18 Holowka, E.; Pochan, D.; Deming, T. *J. Am. Chem. Soc.,* **2005, 127**: 12423

19 Lecommandoux, S.; Achard, M.; Langenwalter, J.; Klok, H. *Macromolecules,* **2001, 34**: 9100

20 Wang, Y.; Chang, Y. *Macromolecules,* **2003, 36**: 6503

21 Andersson, J.; Johannessen, E.; Areva, S.; Baccile, N.; Azais, T.; Lindén, M. *J. Mater. Chem.,* **2007, 17**: 463

22 Andersson, J.; Areva, S.; Spliethoff, B.; Lindén, M. *Biomaterials,* **2005, 26**: 6827